Inorganica Chimica Acta 376 (2011) 73–79

Contents lists available at ScienceDirect

Inorganica Chimica Acta

journal homepage: www.elsevier.com/locate/ica

Insertion reactions of CO_2, OCS, and CS_2 into the Sn–N bonds of $(Me_2N)_2Sn$: NMR and X-ray structural characterization of the products

Constantine A. Stewart [a], Diane A. Dickie [b], Yongjun Tang [b], Richard A. Kemp [a,b,*]

[a] Advanced Materials Laboratory, Sandia National Laboratories, Albuquerque, NM 87106, USA
[b] Department of Chemistry, University of New Mexico, Albuquerque, NM 87131, USA

ARTICLE INFO

Article history:
Received 9 March 2011
Received in revised form 27 May 2011
Accepted 30 May 2011
Available online 6 June 2011

Keywords:
Tin(II) complexes
CO_2 insertion
Carbamate
Thiocarbamate
Dithiocarbamate
X-ray structure

ABSTRACT

The interactions of the heteroallenes CO_2, OCS, and CS_2 with $(Me_2N)_2Sn$ have been investigated. These CX_2 species insert into the Sn–N bonds under mild conditions to provide products bis-(*N*,*N*-dimethylcarbamato)tin(II), $[(Me_2NCO_2)_2Sn]_2$, bis-(*N*,*N*-dimethylthiocarbamato)tin(II), $[Me_2NC(O)S]_2Sn$ and bis-(*N*,*N*-dimethyldithiocarbamato)tin(II), $(Me_2NCS_2)_2Sn$. These molecules have been fully characterized by traditional spectroscopic methods as well as by X-ray crystallography. The $[Me_2NC(O)S]_2Sn$ product is the first example of a structurally characterized Sn(II) thiocarbamate. The solid-state structures of the final products vary depending on the heteroallene inserted. The CO_2-inserted product is dimeric in the solid-state, with both bridging and chelating carbamate ligands. These dimers form a chain-like network via intermolecular Sn···O interactions. The monomeric thiocarbamate also shows a chain-like extended structure, through both Sn···O and Sn···S interactions, while the dithiocarbamate product has no significant intermolecular contacts.

1. Introduction

The reactivity of small, unsaturated molecules such as carbon dioxide with metal amides has been an interest in many research groups [1], including our own [2], over the last several years. While some might propose that the use of CO_2 as a carbon source in the process of preparing industrially important chemicals such as isocyanates and/or carbodiimides would partially alleviate the effects of this greenhouse gas on the environment, the reality is that the quantities involved in chemicals production are miniscule when compared to the daily output of CO_2 in the combustion of fossil fuels. However, a fundamental understanding of how to make the thermodynamically stable CO_2 molecule more reactive in a catalytic cycle could lead to its use as a component in a transportation fuel [3]. In this case, the quantities of CO_2 recycled would be substantial and could offset the release of CO_2 by the combustion of additional fossil fuels.

Carbon dioxide can be considered to have two sites of reactivity. The presence of the two electronegative oxygen atoms causes the carbon to be electron-deficient and prone to nucleophilic attack, while the electron-rich oxygen atoms can act as Lewis bases and are thus susceptible to attack by electrophiles. Similarly, a divalent group 14 metal amide can also be considered to have several sites for reactivity – the nitrogen atoms have lone pairs of electrons making the atoms nucleophilic, while the tin center has both a lone pair of electrons and an empty *p*-orbital, thus making it amphoteric.

While there are many reports in the literature of insertion of CO_2 into transition metal-amide bonds there are far fewer for the CO_2 insertion into the main group metal analogs. In addition to our interest in the reactivity of CO_2 with main group metal amides, we also wanted to investigate a series of reactions using the related heteroallenes OCS and CS_2, as their reactivity can often be dramatically different [4]. In order to gain insight into the fundamental reaction details, pathways and mechanisms of small molecules with metal amides, and to develop new synthetic strategies to produce useful compounds we have chosen to study a simple divalent metal amide – bis(dimethylamido)tin(II), $(Me_2N)_2Sn$ (**1**). Herein, we report on the reactivity of $(Me_2N)_2Sn$ with CO_2, OCS, and CS_2. This work serves as a complement to our recently published report on the interactions of these heteroallenes with silyl-substituted tin(II) amides [4].

These reactions, as will be discussed shortly, produced the inserted products bis-(*N*,*N*-dimethyldicarbamato)tin(II), $[(Me_2NCO_2)_2Sn]_2$ (**2**), bis-(*N*,*N*-dimethylthiocarbamato)tin(II), $[Me_2NC(O)S]_2Sn$ (**3**) and bis-(*N*,*N*-dimethyldithiocarbamato)tin(II), $(Me_2NCS_2)_2Sn$ (**4**). The synthesis of **4** has been reported previously by Perry and Geanangel [5], as has the preparation and crystal structure of the related bis-(*N*,*N*-diethyldithiocarbamato)tin(II) species $(Et_2NCS_2)_2Sn$ (**5**) [6]. However, both prior compounds were prepared by different synthetic routes involving the reactions of $SnCl_2$ and ammonium dithiocarbamate salts [5,6]. We report the

---

* Corresponding author at: Department of Chemistry, University of New Mexico, Albuquerque, NM 87131, USA. Tel.: +1 505 272 7609; fax: +1 505 272 7336.
E-mail address: rakemp@unm.edu (R.A. Kemp).

0020-1693/$ - see front matter © 2011 Elsevier B.V. All rights reserved.
doi:10.1016/j.ica.2011.05.036

direct reaction of $(Me_2N)_2Sn$ with these heteroallenes to prepare the desired products and discuss some of the unusual bonding modes in the crystallographically characterized products using each of these related heteroallenes.

2. Experimental section

2.1. General consideration

All manipulations were carried out in an Ar-filled glove box or by using standard Schlenk techniques [7]. Anhydrous solvents were purchased from Aldrich or Fisher Scientific Company, after which they were stored in the glove box over 4 Å molecular sieves prior to use. ^{1}H, $^{13}C\{^{1}H\}$ and $^{119}Sn\{^{1}H\}$ NMR spectra were obtained on a Bruker AMX 250 spectrometer. The ^{1}H and $^{13}C\{^{1}H\}$ spectra were referenced to residual solvent downfield of $SiMe_4$ while $^{119}Sn\{^{1}H\}$ spectra were referenced to external $SnEt_4$. IR spectra were recorded on a Bruker Vector 22 MIR spectrometer. Melting points were obtained under Ar. Elemental analyses were performed at Columbia Analytical Services, Inc., 3860 S. Palo Verde Road, Tucson, Arizona 85714. While compounds **2**, **3**, and **4** were always handled under Ar, they each possess sufficient stability to be briefly handled in the atmosphere. Although there are no obvious visual changes in color or texture upon exposure to air in the solid state over the course of >24 h, changes in the NMR and IR spectral properties of **2**, **3**, and **4** suggest that these molecules do not tolerate prolonged exposure to the atmosphere.

2.2. X-ray crystallography

Single crystals of **2**, **3**, and **4** were coated with oil and mounted on a CryoLoop™ that had previously been attached using epoxy to a metallic pin. All measurements were made on a Bruker X8 Apex2 CCD-based X-ray diffractometer equipped with an Oxford Cryostream 700 low temperature device and normal focus Mo-target X-ray tube (λ = 0.71073 A) operated at 1500 W power (50 kV, 30 mA).

Data collection and processing were done using the Bruker APEX2 software suite [8]. Structure solution was done by direct methods with the SHELX suite of software [9]. Non-hydrogen atoms were refined anisotropically, while hydrogen atoms were placed in geometrically calculated positions using a riding model. X-ray data are summarized in Table 1.

2.3. $(Me_2N)_2Sn$ (**1**)

$(Me_2N)_2Sn$ was synthesized according to the literature methods [10]. ^{1}H NMR (C_6D_6) δ 2.80 (lit. in C_6H_6 δ 2.75 ppm) and melting point confirmed the product (m.p. = 95–96 °C; lit. m.p. = 91–93 °C); $^{119}Sn\{^{1}H\}$ (C_6D_6) δ 120 ppm.

2.4. $[(Me_2NCO_2)_2Sn]_2$ (**2**)

Under argon, **1** (0.459 g; 2.2 mmol) was dissolved in hexanes (~5 g). Carbon dioxide was bubbled through the pale yellow solution at room temperature for approximately 10 min. After several minutes the reaction turned cloudy. The crude product was collected by filtration and washed with 3 × 25 mL portions of pentane to give 0.629 g of a white solid. This white solid was recrystallized from warm toluene to give **2** as clear, colorless crystals in 97% yield. m.p. = 129–130 °C. *Anal.* Calc. for ($C_6H_{12}N_2O_4Sn$): C, 24.44; H, 4.11; N, 4.50. Found: C, 24.12; H, 4.03; N, 9.64%. ^{1}H NMR ($CDCl_3$) δ 2.88 (s, 3H, CH_3) ppm. $^{13}C\{^{1}H\}$ NMR ($CDCl_3$) δ 36.3 (s, CH_3), 164.5 (s, O–C–O) ppm. $^{119}Sn\{^{1}H\}$ ($CDCl_3$) δ −613 ppm. IR (deposited **2** from a solution of hexanes onto KBr plates and allowed to dry, cm^{-1}) 2359 (s), 2341 (s), 1651 (vw), 1539 (m), 1471 (m), 1384 (vs), 1259 (s), 1019 (s), 793 (w), 668 (m), 648 (m), 548 (s).

Table 1
Crystallographic data and refinement parameters for **2**, **3**, and **4**.

	2	**3**	**4**
Empirical formula	$C_{12}H_{24}N_4O_8Sn_2$	$C_6H_{12}N_2O_2S_2Sn$	$C_6H_{12}N_2S_4Sn$
Formula weight	589.74	327.03	359.11
Crystal size (mm)	0.35 × 0.16 × 0.10	0.45 × 0.10 × 0.07	0.40 × 0.36 × 0.10
Crystal system	monoclinic	monoclinic	monoclinic
Space group	$C2/c$	$P2_1/c$	$C2/c$
T (K)	213(2)	223(2)	223(2)
a (Å)	11.6271(9)	7.8608(6)	8.9253(4)
b (Å)	13.2951(10)	7.4397(5)	12.1265(5)
c (Å)	14.0241(11)	20.1075(14)	12.2492(6)
α (°)	90	90	90
β (°)	111.7980(10)	105.755(4)	109.596(2)
γ (°)	90	90	90
V (Å^3)	2012.9(3)	1131.75(14)	1248.98(10)
Z	4	4	4
Calculated density (g/cm^3)	1.946	1.919	1.910
Absorption coefficient μ (mm^{-1})	2.526	2.599	2.675
Measured reflections	7503	24768	8958
Independent reflections (R_{int})	2354 (0.0196)	4312 (0.0176)	2965 (0.0265)
R_1, wR_2 (all data)	0.0228, 0.0539	0.0216, 0.0663	0.0337, 0.0729
R_1, wR_2 [$I > 2\sigma(I)$]	0.0216, 0.0532	0.0172, 0.0529	0.0250, 0.0663
GOF on F^2	1.119	1.324	1.041

2.5. $[Me_2NC(O)S]_2Sn$ (**3**)

Under argon, **1** (1.062 g; 5.1 mmol) was dissolved in hexanes (4 g) and added to a heavy walled glass reactor tube fitted with a 74 cc stainless steel bomb. The pale yellow hexanes solution of **1** was cooled to −78 °C and the system evacuated to remove argon. The 74 cc bomb was charged with carbonyl sulfide to a pressure of 60 psig (~5 atm) and then condensed into the heavy walled glass reactor. Another 60 psig was charged to the 74 cc bomb and condensed into heavy walled glass reactor tube and a final 22 psig of OCS was charged to the bomb and condensed into the tube. The cumulative charges of OCS amounted to 31 mmol. Once all of the OCS was condensed into the heavy walled glass reactor tube at −78 °C the system pressure read <0 psig. The reaction was allowed to slowly warm to room temperature while stirring over a period of 12 h. During that time, the pressure of the system was ~12 psig. The reaction vessel was then vented; the crude product was collected by filtration and washed with three portions of pentane (~25 mL) to give 1.385 g of a white solid (crude yield = 83%). This white solid was recrystallized from hexanes to give **3** as white crystals. m.p. = 154–156 °C. *Anal.* Calc. for ($C_6H_{12}N_2O_2S_2Sn$): C, 22.04; H, 3.70; N, 8.57. Found: C, 21.65; H, 3.42; N, 8.32%. ^{1}H NMR ($CDCl_3$) δ 2.92 (s, 3H, CH_3), 3.05 (s, 3H, CH_3) ppm. $^{13}C\{^{1}H\}$ NMR ($CDCl_3$) δ 35.7 (CH_3), 39.6 (CH_3), 181.4 (O–C–S) ppm. $^{119}Sn\{^{1}H\}$ ($CDCl_3$) δ −351 ppm. IR (Nujol mull, KBr plates, cm^{-1}) 2066 (w), 547 (m), 1530 (m), 1180 (vw), 965 (m), 1018 (s), 800 (vw), 699 (m).

2.6. *($Me_2NCS_2)_2Sn$* (**4**)

Under argon, **1** (0.285 g; 1.4 mmol) was dissolved in ether (10 g). To this stirring solution at room temperature was added CS_2 (0.35 mL; 5.8 mmol) drop-wise via syringe. An immediate, exothermic reaction occurred to produce a yellow precipitate. The volatiles were removed under vacuum to give a pale yellow powder (0.385 g, crude yield = 77%, m.p. = 244–246 °C dec.). The crude product was recrystallized from hot dimethyl sulfoxide to give pale yellow crystals of **4**. m.p. = 245 °C; lit. 185 °C dec. [5]. *Anal.* Calc. for ($C_6H_{12}N_2S_4Sn$): C, 20.07; H, 3.37; N, 7.80. Found: C, 20.06; H, 3.20; N, 7.80%. ^1H NMR ($CDCl_3$) δ 3.38 (s, CH_3) ppm; (in C_6D_6) δ 2.57 (s, CH_3) ppm; $^{13}C\{^1H\}$ NMR ($CDCl_3$) δ 42.7 (CH_3), 201.4 (S–C–S) ppm. $^{119}Sn\{^1H\}$ ($CDCl_3$) δ −556 ppm. IR (Nujol mull, KBr plates, cm^{-1}) 1520 (m), 1244 (m), 1148 (m), 1018 (m), 965 (m), 722 (m), 572 (m).

3. Results and discussion

The reactions of **1** with CO_2, OCS, and CS_2 were straightforward and involved insertion of the heteroallene into the Sn–N bonds to provide $[(Me_2NCO_2)_2Sn]_2$ **2**, $[Me_2NC(O)S]_2Sn$ **3**, and $(Me_2NCS_2)_2Sn$ **4**, respectively (Scheme 1). The reactions with CO_2 and CS_2 took place under exceedingly mild conditions at room temperature. The reaction with OCS was accomplished by condensing the gas into the reactor at low temperature (−78 °C) and allowing the reaction to warm to room temperature. The yields for these reactions to produce analytically pure products ranged from 77% for **4** to 97% for **2**. Elemental analysis, NMR and IR spectroscopies, and single crystal X-ray diffraction were all used to characterize the products from these reactions. X-ray diffraction results were particularly useful in studying the solid-state structure of the products and revealed some peculiar features in the intermolecular interactions, discussed in more detail below.

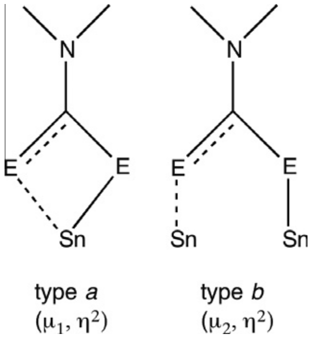

Fig. 1. Two types of bonding observed for Me_2NCE_2 with Sn(II); type *a* – terminal bidentate (chelating) and type *b* – bridging bidentate.

The geometry and bonding of the Me_2NCE_2 ligands in these carbamato compounds can be described as either type *a* or type *b*, as seen in Fig. 1 [2a]. In type *a* bonding the Me_2NCE_2 ligand is terminal bidentate (chelating), while in type *b* bonding the Me_2NCE_2 ligand is bridging bidentate. As will be seen, we have observed both types *a* and *b* bonding modes in **2** while only type *b* bonding is present in complexes **3** and **4** (*vide infra*).

For the preparation of **2**, CO_2 was bubbled through a hexanes solution of compound **1** at atmospheric pressure and room

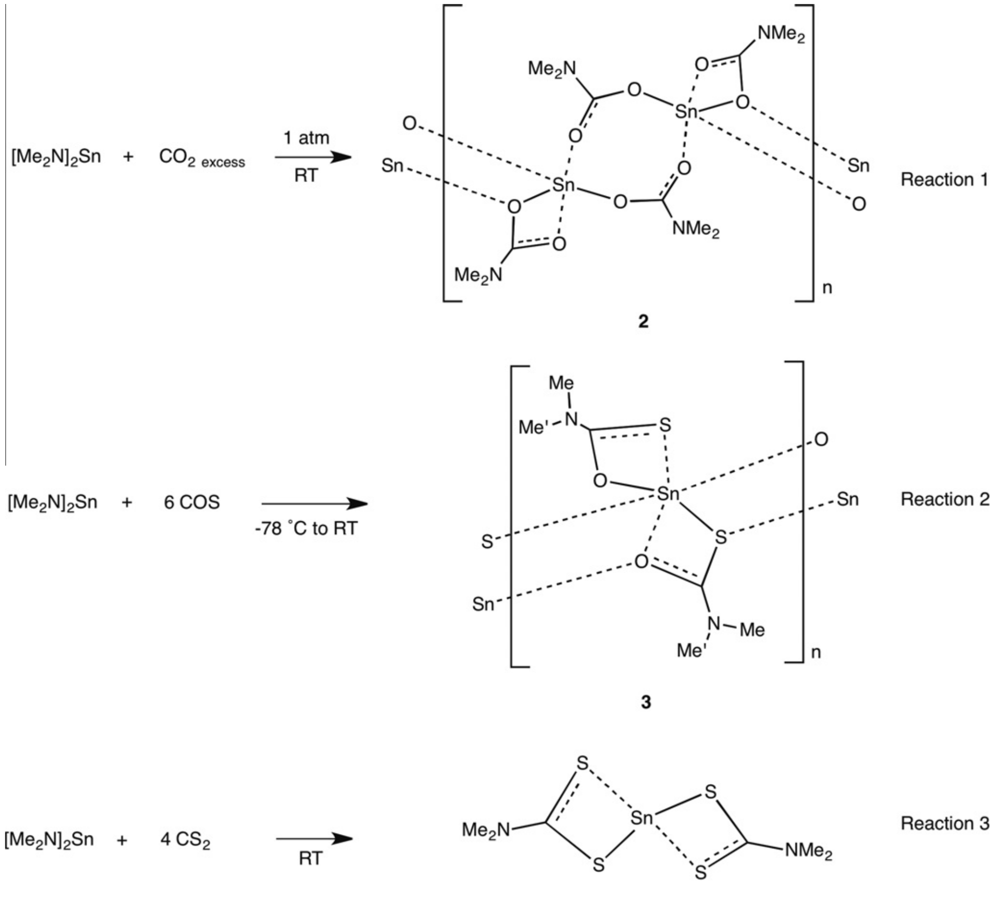

2

3

4

Scheme 1.

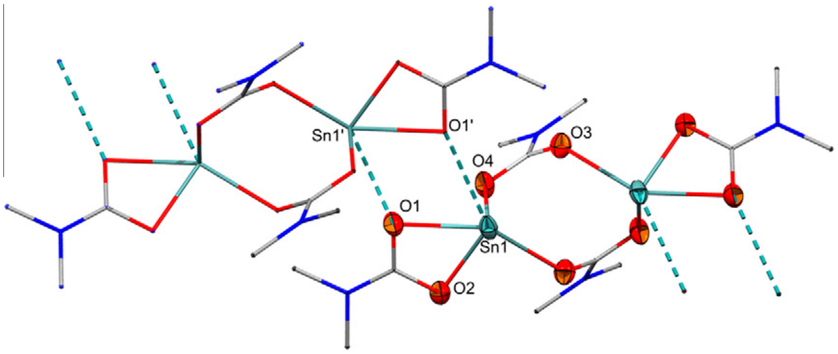

Fig. 2. Molecular structure of **2** (50% ellipsoids). For clarity, hydrogen atoms are not shown and the dimethylamino groups are shown as sticks. Close interaction between neighboring molecules: Sn(1)···O(1), 2.8499(18) Å. Selected bond lengths (Å) and angles (°): Sn(1)–O(1) 2.3320(17), Sn(1)–O(3) 2.4323(15), Sn(1)–O(2) 2.3352(18), Sn(1)–O(4) 2.1152(16); O(1)–Sn(1)–O(3) 137.92(6), O(2)–Sn(1)–O(4) 86.18(7).

temperature (see Scheme 1, reaction 1). The reaction was slightly exothermic and produced very small, white crystals of **2**. Compound **2** was fully characterized by ^{1}H, ^{13}C{^{1}H}, ^{119}Sn{^{1}H}, and IR spectroscopies, as well as single crystal X-ray diffraction. The ^{1}H NMR spectrum exhibited one resonance for the methyl groups at δ 2.88 ppm. The ^{13}C{^{1}H} NMR spectrum displayed the expected two singlets, one at δ 36.3 ($-CH_3$ groups) and another at δ 164.5 ppm (Me_2NCO_2- carbons). The NMR results suggested a simple insertion of CO_2 into the Sn–N bond to form the symmetrically coordinated carbamato group. The ^{13}C{^{1}H} resonance for the carbamato carbons in **2** is similar to that reported by Calderazzo and co-workers at 22 °C for the $Al_2(O_2CN^iPr_2)_6$ carbamato carbons (δ 163.5 ppm in $CDCl_3$), which has both bridging and terminal carbamato ligands [11]. However, at −55 °C they observed two peaks for the carbamato resonances (δ 165.4 $O_2CN_{terminal}$; δ 158.6 $O_2CN_{bridging}$). Based on their ambient and low temperature NMR observations, we knew that we could not rule out **2** being dimeric and possessing both bridging and terminal carbamato ligands. The IR spectrum of **2** (film on KBr plates) exhibited absorbances below 1600 cm^{-1}, which is suggestive of a compound containing both bridging and terminal bidentate carbamate groups according to Calderazzo and co-workers [11]

A single crystal X-ray diffraction study revealed that in fact **2** exists as a dimer in the solid-state, and that both type *a* and *b* carbamato ligands are bound to the tin centers as shown in Fig. 2. Based on our search of the literature and the Cambridge Structural Database (CSD, version 5.32) [12] this is the first structurally characterized homoleptic Sn(II) carbamate to be reported. One other heteroleptic Sn(II) carbamate was recently reported by us [4], and two homoleptic Sn(IV) carbamates $[(R_2NCO_2)_4Sn$, R = Et, ^{i}Pr] are also known [13]. Examination of the structure shows that the bidentate carbamate groups occupy both bridging and terminal roles. For the bridging carbamate ligand the O(3)–C(4)–O(4) bond angle is 121.8(2)°, and as would be expected this angle is slightly greater than the terminal O(2)–C(1)–O(1) bond angles of 118.9(2)°. The two C–O bond distances of the terminal bidentate carbamate ligands are the same length within experimental error – C(1)–O(2) 1.280(3) Å and C(1)–O(1) 1.272(3) Å, suggesting near-complete charge delocalization. The C–O bond lengths for the bridging bidentate carbamate ligand exhibit both short and long C–O bond distances, with a shorter C(4)–O(3) bond length of 1.263(3) Å and a longer one, C(4)–O(4), of 1.295(3) Å. As with Sn(IV) carbamates, the shorter C–O bonds are also the ones that are associated with the longer Sn–O bonds [13]. We note that the η^2 chelation mode exhibited by the terminal ligand is significantly less common in both carbamates and carboxylates relative to bridging modes when bound to main group metals (M). This finding has been previously attributed to the reluctance of a highly strained, four-membered MO_2C ring to form in the presence of the two electron-rich oxygen atoms of the chelating ligand [1e,2a]. Thus, the tendency is for the ligand to reduce electron density at the metal by forming bridges to multiple metals, resulting in a more stable binding mode. Substitution of one or both of the highly donating oxygen atoms with less electron-rich atoms such as sulfur render the chelating mode much more favorable.

The local geometric environment around the two Sn atoms in **2** can best be described as a highly distorted trigonal bipyramidal (*tbp*) structure (*vide infra*). In addition, compound **2** exhibits close

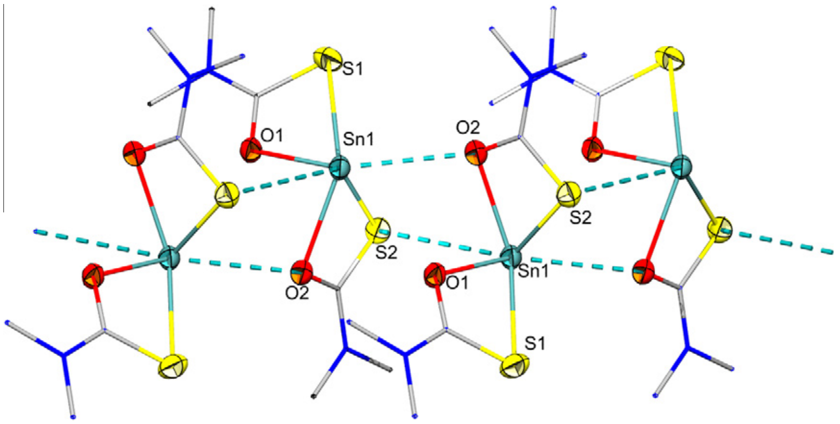

Fig. 3. Molecular structure of **3** (50% ellipsoids). For clarity, hydrogen atoms are not shown and the dimethylamino groups are shown as sticks. Close interactions between neighboring molecules: Sn(1)···S(2), 3.3900(5) Å and Sn(1)···O(2), 2.9706(11) Å. Selected bond lengths (Å) and angles (°): Sn(1)–O(2) 2.4231(12), Sn(1)–S(1) 2.7650(5), Sn(1)–O(1) 2.2196(11), Sn(1)–S(2) 2.6070(5); S(1)–Sn(1)–O(2) 134.46(3), S(2)–Sn(1)–O(1) 89.54(3).

Sn···O interactions of 2.8499(18) Å between the Sn(1) and O(1) atoms of neighboring molecules to give an extended chain-like polymeric network in the solid state.

The reaction of **1** with OCS was conducted under slightly different conditions. In this case **1** was dissolved in hexanes, placed in a heavy walled glass vessel, cooled to −78 °C, evacuated, and the reaction vessel charged with an excess of OCS (~31 mmol). Work-up of the reaction and purification of the crude product by crystallization from hexanes gave compound **3** in very good isolated yield (83%). The ^1H NMR spectrum of **3** exhibited singlets at δ 2.92 and 3.05 ppm, suggesting the existence of nonequivalent methyl groups on the thiocarbamate ligand [Me′(Me)NC(O)S]−. The $^{13}C\{^1H\}$ NMR spectrum showed three resonances at δ 35.7, 39.6, and 181.4 ppm for the non-equivalent methyl groups and the thiocarbamate carbon, respectively. The $^{13}C\{^1H\}$ shift of the carbon of the $[Me_2NC(O)S]$– group for **3** is similar to other homoleptic main-group thiocarbamates – e.g., $[Et_2NC(O)S]_3In$ (δ 182.4 ppm [14]) and $[^iPr_2NC(O)S]_3In$ (δ 181.4 ppm [15]). Both of these indium-containing complexes were prepared via the metathesis reaction of stoichiometric quantities of $InCl_3$ and the lithium dialkylthiocarbamate salts and not by the direct insertion of OCS. As well, these complexes were described as being only sparingly soluble in most organic solvents.

The reason for the two distinct, non-equivalent methyl group resonances for **3** in both the ^1H and $^{13}C\{^1H\}$ NMR spectra were also supported by the single crystal X-ray diffraction results, as shown in Fig. 3. In contrast to **2**, the thiocarbamate ligands of **3** chelate rather than bridge, and **3** exists as a monomer. A search of the CSD [12] showed that compound **3** appears to be the first structurally-characterized thiocarbamate Sn(II) complex, although Sn(IV) complexes of thiocarbamates based on pyrrole or morpholine made via routes other than OCS insertion are known and have been structurally characterized [16].

The geometric environment of the Sn atom in compound **3** can best be described as a highly distorted *tbp* structure with a stereoactive lone pair of electrons occupying an equatorial position at the formally Sn(II) center. This distorted *tbp* environment is expected based on the discussions present in reviews by Heard [17] and Tiekink [18] about dithiocarbamate complexes. The stereoactive lone pair of electrons forces the O(2)–Sn(1)–S(1) bond angle to distort to 134.46(3)°, significantly wider than in other main group thiocarbamates (116–120°) [14–16,19]. Comparing the bond distances of the four atoms attached to Sn(1) – (S(1), S(2), O(1) and O(2) – the atoms S(1) and O(2) can be assigned the axial positions due to their longer Sn–O bonds, Sn(1)–S(1) 2.7650(5) Å and Sn(1)–O(2) 2.4231(12) Å. The comparatively shorter Sn(1)–S(2) and Sn(1)–O(1) bond distances of 2.6070(5) and 2.2196(11) Å, respectively, places the S(2) and O(1) atoms in the equatorial positions.

For related main group thiocarbamates, the M–S and M–O bonds range in length from 2.44–2.77 and 2.24–2.81 Å, respectively. This assignment of the longer bonds to the axial positions and shorter ones to the equatorial positions is consistent with descriptions of the bonding in tin(II) dithiocarbamates [17,18] as well as an indium thiocarbamate [14]. The axial and equatorial assignments for these four atoms are also manifest in their comparatively shorter $C(1)–S(1)_{ax}$ and $C(2)–O(2)_{ax}$ bonds (1.7369(17) and 1.2623(19) Å, respectively) versus the somewhat longer $C(2)–S(2)_{eq}$ and $C(1)–O(1)_{eq}$ bonds (1.7552(17) and 1.2815(18) Å, respectively). As with the M–O and M–S bonds, these bonds are on the edge of the range of comparable main group thiocarbamates (C–S = 1.73–1.78 Å; C–O = 1.22–1.27 Å).

Close inspection of the packing of compound **3** shows that the nearest interactions between adjacent molecules are Sn(1)–S(2), 3.3900(5) Å and Sn(1)–O(2), 2.9706(11) Å. These distances are all outside the sum of the covalent radii of the atoms ($Sn_{covalent\ radius}$ = 1.39 Å; $S_{covalent\ radius}$ = 1.05 Å; $O_{covalent\ radius}$ = 0.66 Å), but within the van der Waals radii sums ($Sn_{van\ der\ Waals}$ = 2.17 Å; $S_{van\ der\ Waals}$ = 1.80 Å; $O_{van\ der\ Waals}$ = 1.52 Å). These close Sn···S intermolecular distances in **3** suggest an extended network in the solid state, similar to that found in **2**. However, even with this extended network, in contrast to the indium thiocarbamates [14,15] **3** is surprisingly soluble in hexanes and chloroform.

The last reaction in this series is between **1** and CS_2 to give $(Me_2NCS_2)_2Sn$ (**4**). We noted that **4** has been reported previously by Perry and Geanangel [5], although prepared in 45% yield via the reaction of ammonium dithiocarbamate salts with $SnCl_2$. We prepared **4** by reacting of a solution of **1** in diethyl ether with a slight excess of CS_2. The reaction was immediate and exothermic, and produced a yellow precipitate isolated in 77% yield. The product was largely insoluble in common solvents (e.g., CH_2Cl_2, THF, toluene, ether, hexanes, or benzene) and was purified by recrystallization from hot dimethyl sulfoxide. Compound **4** was only slightly soluble in $CDCl_3$ and C_6D_6, which made obtaining the $^{13}C\{^1H\}$ NMR spectrum challenging. It is interesting to note that Perry and Geanangel reported two singlets in the ^1H NMR spectrum (in C_6H_6) at δ 3.04 and 2.90 ppm, which they postulated were due to restricted rotation about the C–N bond. However, we observed only a single resonance at δ 3.38 ppm for **4** in the proton NMR spectrum ($CDCl_3$). Their reported observation of the two resonances for the methyl groups prompted us to reevaluate the ^1H spectra of **4** in C_6D_6 to see if the two singlets were due to solvent or polarity effects. Therefore, we prepared a sample of **4** in C_6D_6 and again observed only a single resonance in the ^1H NMR spectrum, although this time it was found at δ 2.57 ppm. As mentioned previously, **4** was only sparing soluble in most solvents, which presented some difficulty when trying to obtain the $^{13}C\{^1H\}$ NMR spectrum. The methyl groups on Me_2NCS_2 group exhibited a single resonance at δ 42.7 ppm. However, only a very weak signal for the carbon of the dithiocarbamate could be observed at δ 201.4 ppm, as listed in Table 2. This resonance at δ 201.4 ppm for the dithiocarbamate carbon of Me_2NCS_2– is comparable to that reported by van Gaal and co-workers for $(Et_2NCS_2)_2Sn$ (**5**) at δ 199.9 ppm in $CDCl_3$ [20].

Comparisons of the NMR spectra of **2**, **3**, and **4** deserve added discussion. As can be seen from Table 2, there is a smooth downfield shift for the ^1H and ^{13}C resonances with the increase in the number of sulfur atoms in the complexes. In particular, the carbon resonance in the Me_2NCE_2– group becomes more deshielded as sulfur atoms replace oxygen atoms in the carbamate group. This downfield shift tracks well with the ^{13}C shifts of the carbon in CO_2, OCS, and CS_2 (δ 124.2, 153.8, and 192.6 ppm, respectively). However, there appears to be no corresponding order to the chemical shifts in the ^{119}Sn NMR spectra for compounds **2**, **3**, and **4**.

The structure of **4** was verified by single crystal X-ray diffraction and is shown in Fig 4. Compound **4** is unique in this series in that there are no extended intermolecular interactions in the solid-state between the Sn and S atoms. In this case the shortest intermolecular tin–sulfur distance is 4.059 Å, which is outside the sum of the van

Table 2
^1H, $^{13}C\{^1H\}$ and $^{119}Sn\{^1H\}$ NMR chemical shifts for **2**, **3**, and **4**.

Compound	^1H [a]	$^{13}C\{^1H\}$ [b]	$^{119}Sn\{^1H\}$ [c]
2	2.88 (CH_3)	36.3 (CH_3) 164.5 (O–*C*–O)	−613
3	2.92 (CH_3) 3.05 (CH_3)	35.7 (CH_3) 39.6 (CH_3) 181.4 (O–*C*–O)	−351
4	3.38 (CH_3)	42.7 (CH_3) 201.4 (O–*C*–O)	−556

[a] ($CDCl_3$; Ref. Me_4Si), ppm.
[b] ($CDCl_3$; Ref. Me_4Si), ppm.
[c] ($CDCl_3$; Ref. Et_4Sn), ppm.

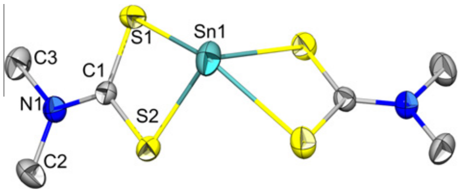

Fig. 4. Molecular structure of **4** (50% ellipsoids). For clarity, hydrogen atoms are not shown. Selected bond lengths (Å) and angles (°): Sn(1)–S(1) 2.7514(4), Sn(1)–S(2) 2.5722(4); S(1)–Sn(1)–S(2), 88.630(12), S(1)–C(1)–N(1) 121.60(9), S(2)–C(1)–N(1) 120.34(9), S(1)–C(1)–S(2) 118.05(7).

der Waals' radii of Sn and S ($Sn_{van\ der\ Waals}$ = 2.17 Å; $S_{van\ der\ Waals}$ = 1.80 Å). While Sn(IV) thiocarbamate complexes are ubiquitous and have been recently reviewed [17,18], there are only two dithiocarbamate Sn(II) structures reported in the literature that have similar structures to **4**. These two structures are both of $(Et_2NCS_2)_2Sn$ (**5**), reported by Potenza and Mastropaolo in 1973 [6a], and by Hoskins et al. in 1976 [6b]. Potenza and Mastropaolo describe **5** as consisting of essentially discrete monomeric units; however, they do point out that the Sn and S atoms of neighboring molecules are at a distance of 3.849 Å, just within the sum of the van der Waals radii (3.97 Å) for these two atoms (Fig. 5). For structural comparisons between **4** and **5** we chose to use the X-ray metrical data from Hoskins et al. due to the higher quality of the structure as seen by the lower *R*-factor value.

The geometry around the Sn atom in **4**, as found in compound **3**, is best described as distorted *tbp* in nature. The $S(1)_{ax}$–Sn(1)–$S(1)_{ax}$ bond angle in **4** (142.26(2)°) is slightly larger than that found in **5** (139.64°). The longer Sn(1)–$S(1)_{ax}$ bonds for **4** are associated with the shorter C(1)–S(1) bonds (1.7092(12) Å), while the shorter Sn(1)–$S(2)_{ax}$ bonds are attached to S(2) bound to the longer C(1)–S(2) bonds (1.7349(12) Å). In compound **4** the $S(2)_{eq}$–Sn(1)–$S(2)_{eq}$ angle is 101.306(18)°, larger than the S_{eq}–Sn–S_{eq} angle found in **5** (96.05°). The Sn(1)–$S(1)_{ax}$ bond in **4** is 2.7514(4) Å, while in **5** the two Sn–S_{ax} bond lengths are 2.768 and 2.882 Å. It is noteworthy that both Sn–S axial bonds in **4** are shorter than those axial bonds in **5**. Recall there are no Sn interactions with other atoms of neighboring molecules in **4**. This may be the reason for the slightly longer Sn–S_{ax} bond lengths in **5** as compared to **4**. The Sn atom in **5** is receiving electron density from a sulfur atom of a neighboring molecule, likely causing a slight lengthening of its internal Sn–S_{ax} bond distances.

4. Conclusions

The reaction of $(Me_2N)_2Sn$ **1** with CO_2, OCS, and CS_2 all provide insertion of the CE_2 moiety into the Sn–N bonds to give **2**, **3**, and **4**, respectively. The localized geometry at the tin center of all of these complexes can best be described as a distorted *tbp* structure with the tin center containing a stereoactive lone pair of electrons. The major difference among these compounds is that $[(Me_2NCO_2)_2Sn]_2$ **2** is a dimer while complexes **3** and **4** are monomers in the solid-state. Compound **2** exhibits both bridging and terminal carbamate ligands and is somewhat surprisingly the first structurally characterized Sn(II) dialkylcarbamate. Because of the close intermolecular interactions between neighboring Sn and O atoms in the solid state, **2** can be described as a loosely-coordinated polymer. The reaction of **1** with OCS yielded $[Me_2NC(O)S]_2Sn$ **3**. In this case complex **3** is a monomer, and is also the first example of a structurally characterized thiocarbamate Sn(II) complex. However, in the solid-state the structure for **3** exhibits some extended intermolecular interactions between the Sn···O and Sn···S atoms of neighboring molecules, forming a coordination polymer similar to **2**. Lastly, compound **4**, prepared from **1** and CS_2, is also monomeric in the solid state; however, there are no close interactions between tin and any neighboring S atoms.

Acknowledgments

This work was financially supported by the National Science Foundation (Grant CHE09-11110) and by the Laboratory Directed Research and Development (LDRD) program at Sandia National Laboratories (LDRD 14938 and 151300). The Bruker X-ray diffractometer was purchased via a National Science Foundation CRIF:MU award to the University of New Mexico (CHE-0443580). Sandia is a multiprogram laboratory operated by Sandia Corporation, a Lockheed Martin Company, for the United States Department of Energy under Contract No. DE-AC04-94AL85000.

Appendix A. Supplementary material

CCDC 806650, 806651, and 806652 contain the supplementary crystallographic data for compounds (**2**), (**3**), and (**4**), respectively. These data can be obtained free of charge from The Cambridge Crystallographic Data Centre via www.ccdc.cam.ac.uk/data_

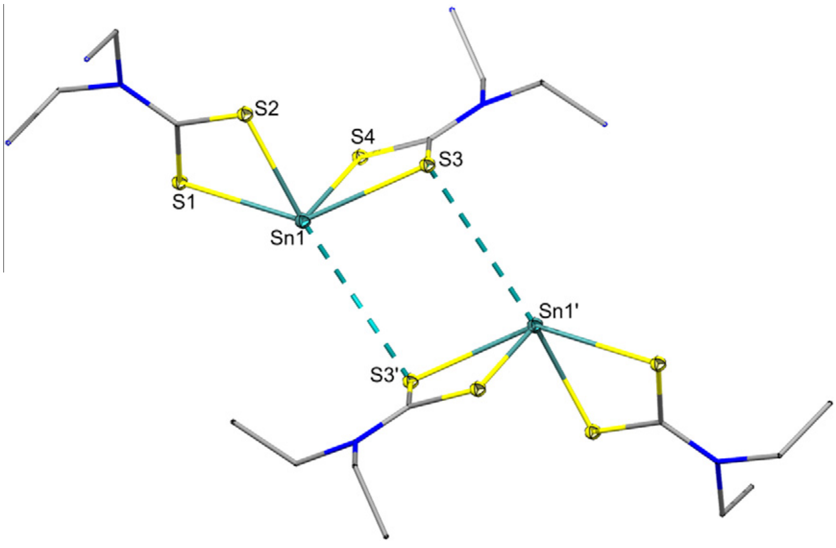

Fig. 5. Molecular structure of **5** (50% ellipsoids). For clarity, hydrogen atoms are not shown and diethylamino groups are shown as sticks. Close interactions between neighboring molecules: Sn(1)···S(3)′ 3.849 Å.

request/cif. Supplementary data associated with this article can be found, in the online version, at doi:10.1016/j.ica.2011.05.036.

References

[1] (a) U. Wannagat, H. Kuckertz, C. Krueger, J. Pump, Z. Anorg. Allg. Chem. 333 (1964) 54;
(b) L.R. Sita, J.R. Babcock, R. Xi, J. Am. Chem. Soc. 118 (1996) 10912;
(c) D. Belli Dell'Amico, F. Calderazzo, L. Labella, F. Marchetti, G. Pampaloni, Chem. Rev. 103 (2003) 3857;
(d) C.-C. Chang, B. Srinivas, W. Mung-Liang, C. Wen-Ho, M.Y. Chiang, H. Chung-Sheng, Organometallics 14 (1995) 5150;
(e) K.-C. Yang, C.-C. Chang, C.-S. Yeh, G.-H. Lee, S.-M. Peng, Organometallics 20 (2001) 126;
(f) M.T. Caudle, R.A. Nieman, V.G. Young Jr., Inorg. Chem. 40 (2001) 1571;
(g) H.-J. Himmel, Z. Anorg. Allg. Chem. 633 (2007) 2191;
(h) M. Kahnes, H. Görls, M. Westerhausen, Z. Anorg. Allg. Chem. (2011), doi:10.1002/zaac.201000397.

[2] (a) Y. Tang, L.N. Zakharov, A.L. Rheingold, R.A. Kemp, Organometallics 23 (2004) 4788;
(b) Y. Tang, W.S. Kassel, L.N. Zakharov, A.L. Rheingold, R.A. Kemp, Inorg. Chem. 44 (2005) 359;
(c) Y. Tang, A.M. Felix, V.W. Manner, L.N. Zakharov, A.L. Rheingold, B. Moasser, R.A. Kemp, ACS Symp. Ser. 917 (2006) 410;
(d) D.A. Dickie, M.V. Parkes, R.A. Kemp, Angew. Chem., Int. Ed. 47 (2008) 9955.

[3] (a) Y. Ono, Appl. Catal., A 155 (1997) 133;
(b) J. Louie, Curr. Org. Chem. 9 (2005) 605;
(c) D. Ballivet-Tkatchenko, R. Burgat, S. Chambrey, L. Plasseraud, P. Richard, J. Organomet. Chem. 691 (2006) 1498;
(d) D. Ballivet-Tkatchenko, S. Chambrey, R. Keiski, R. Ligabue, L. Plasseraud, P. Richard, H. Turunen, Catal. Today 115 (2006) 80;
(e) D. Ballivet-Tkatchenko, H. Chermette, L. Plasseraud, O. Walter, Dalton Trans. (2006) 5167;
(f) T. Sakakura, J.-C. Choi, H. Yasuda, Chem. Rev. 107 (2007) 2365;
(g) M. Aresta, A. Dibenedetto, Dalton Trans. (2007) 2975;
(h) M. Aresta, A. Dibenedetto, F. Nocito, C. Pastore, Inorg. Chim. Acta 361 (2008) 3215;
(i) J.-C. Choi, K. Kohno, Y. Ohshima, H. Yasuda, T. Sakakura, Catal. Commun. 9 (2008) 1630.

[4] C.A. Stewart, D.A. Dickie, M.V. Parkes, J.A. Saria, R.A. Kemp, Inorg. Chem. 49 (2010) 11133.

[5] D. Perry, R.A. Geanangel, Inorg. Chim. Acta 13 (1975) 185.

[6] (a) J. Potenza, D. Mastropaolo, Acta Crystallogr., Sect. B: Struct. Sci. 29 (1973) 1830;
(b) B.F. Hoskins, R.L. Martin, N.M. Rohde, Aust. J. Chem. 29 (1976) 213.

[7] D.F. Shriver, M.A. Drezdzon, The Manipulation of Air-Sensitive Compounds, second ed., Wiley Interscience, New York, 1986.

[8] Bruker, in: Bruker AXS, Inc., Madison, Wisconsin, USA, 2007.

[9] G.M. Sheldrick, Acta Crystallogr., Sect. A 64 (2008) 112.

[10] P. Foley, M. Zeldin, Inorg. Chem. 14 (1975) 2264.

[11] D. Belli Dell'Amico, F. Calderazzo, M. Dell'Innocenti, B. Güldenpfennig, S. Ianelli, G. Pelizzi, P. Robino, Gazz. Chim. Ital. 123 (1993) 283.

[12] F.H. Allen, Acta Crystallogr., Sect. B: Struct. Sci. 58 (2002) 380.

[13] (a) L. Abis, D. Belli Dell'Amico, F. Calderazzo, R. Caminiti, F. Garbassi, S. Ianelli, G. Pelizzi, P. Robino, A. Tomei, J. Mol. Catal. A: Chem. 108 (1996) L113;
(b) G.A. Horley, M.F. Mahon, K.C. Molloy, P.W. Haycock, C.P. Myers, Inorg. Chem. 41 (2002) 5052.

[14] G.A. Horley, M. Chunggaze, P. O'Brien, A.J.P. White, D.J. Williams, J. Chem. Soc., Dalton Trans. (1998) 4205.

[15] G.A. Horley, P. O'Brien, J.-H. Park, A.J.P. White, D.J. WIlliams, J. Mater. Chem. 9 (1999) 1289.

[16] (a) D.K. Srivastava, V.D. Gupta, H. Noth, W. Rattay, J. Chem. Soc., Dalton Trans. (1988) 1533;
(b) S. Chandra, B.D. James, R.J. Magee, W.C. Patalinghug, B.W. Skelton, A.H. White, J. Organomet. Chem. 346 (1988) 7.

[17] P.J. Heard, Prog. Inorg. Chem. 53 (2005) 1.

[18] E.R.T. Tiekink, Appl. Organomet. Chem. 22 (2008) 533.

[19] J.S. Casas, A. Castineiras, A. Sanchez, J. Sordo, E.M. Vazquez-Lopez, Main Group Met. Chem. 19 (1996) 231.

[20] H.L.M. Van Gaal, J.W. Diesveld, F.W. Pijpers, J.G.M. Van der Linden, Inorg. Chem. 18 (1979) 3251.